Chapter 2

The CDF detector

This study is performed using the data collected by the Collider Detector at Fermilab (CDF) during 1994–1995 (RUN1B). The CDF is a multi-purpose detector built at the B0 collision point of the Tevatron Collider which gives a head-on collision of the proton and the anti-proton with the center of mass energy of 1800 GeV. Figure 2.1 shows a schematic view of the CDF. The main component of the CDF detector is categorized into two sub-systems, a tracking system (SVX,VTX,CTC and the superconducting solenoidal magnet) and a calorimeter system (Forward,Plug,Wall,Central). Each of those sub-systems is arranged to be symmetric in the cylindrical direction. In this chapter each sub-system of the CDF detector is briefly described with emphasis on what we used in our analysis. The full description of the CDF detector is found in the reference [15].

2.1 Coordinate system

Overall CDF coordinate $(x, y, z, r, \phi, \theta)$

We describe the coordinate system and the notation used in the thesis. Figure 2.2 shows the overall CDF coordinate system. In the CDF coordinate system, the origin is at the center of the central tracking chamber (CTC). The beam axis is taken as the z axis and positive in the proton direction.

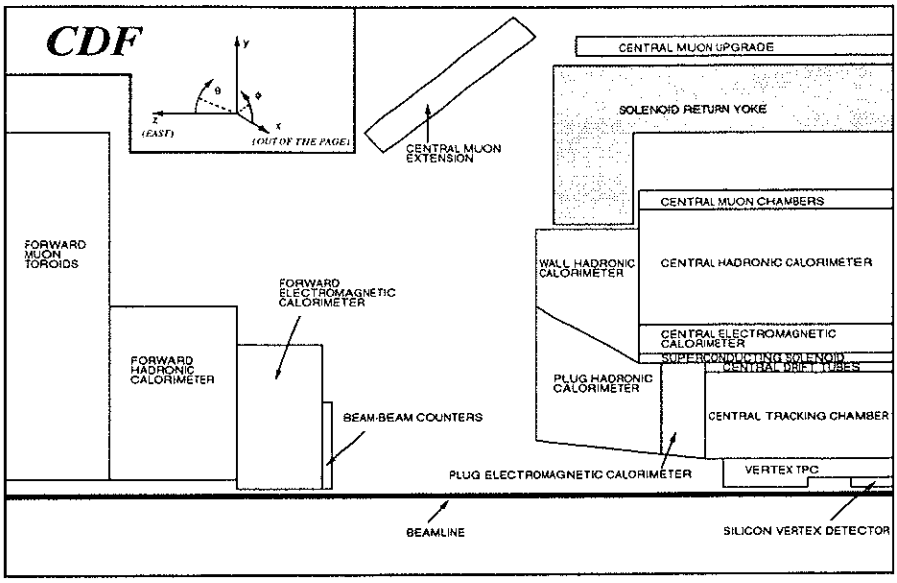

Figure 2.1: A quarter view of the CDF detector.

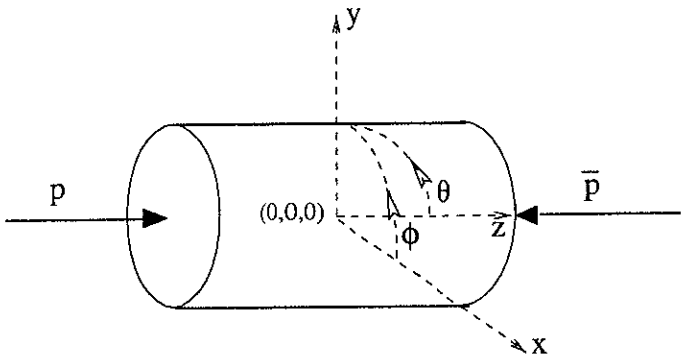

Figure 2.2: The CDF coordinate system.

The y axis is vertical and positive in upward. The x axis is horizontal and the direction is defined by the right-handed coordinate system.

The cylindrical coordinate system is also used. The r indicates the radial distance from the z-axis. The azimuthal angle about z-axis is represented by the ϕ, and defined 0 at x-axis. The polar angle relative to z-axis is represented by the θ, and defined 0 at z-axis.

Track parameterization $(\cot\theta, C, z_0, d, \phi_0)$

The CDF has a solenoidal magnet which functions as a spectrometer magnet in the central region of the CDF. Under this magnetic field, a trajectory of charged particle become a helix, the axis of which is parallel to the magnetic field. At the CDF the following 5 parameters are used to describe the helix of a track [16]:

$$\vec{\alpha} = (\cot\theta, C, z_0, d, \phi_0)$$

where:

$cot\theta$	:	cotangent of the polar angle at minimum approach.
C	:	half curvature
z_0	:	z position at point of minimum approach to origin of helix.
d	:	signed impact parameter distance between helix and origin at minimum approach.
ϕ_0	:	azimuthal angle of track at point of minimum approach.

Pseudorapidity (η), Transverse energy (E_T)

In a hadron-hadron collision, interacting system is variously boosted along z-direction in event by event. It is thus convenient to use an invariant form under Lorentz boost to describe the physical quantity, such as a cross section. Consider the invariant volume element in the momentum space,

$$\frac{dp_x\, dp_y\, dp_z}{E}.$$

This form is invariant to any Lorentz transformation. Since the CDF is a symmetric detector in ϕ direction, this form can be transformed into the following expression in the cylindrical coordinate,

$$\frac{\pi p_T \, dp_T \, dp_z}{E}.$$

where p_T is defined as $p_T \equiv p \sin\theta$. Against the Lorentz boost along the z-direction, p_T and dp_T are obviously invariant. Since the overall expression is an invariant form, the rest term, dp_z/E is an invariant quantity for z-boost. It is thus useful to introduce the new variable y by the following differential equation,

$$dy \equiv \frac{dp_z}{E} = \frac{dp_z}{\sqrt{m^2 + {p_T}^2 + {p_z}^2}}.$$

Solving this equation, y is defined as,

$$y \equiv \frac{1}{2} \ln \left(\frac{E + p_z}{E - p_z} \right).$$

This value is called *rapidity* of the particle. The shape of rapidity distribution dN/dy is invariant under z-boost.

For $p \gg m$, the rapidity may be approximated by the *pseudorapidity*,

$$\eta \equiv \frac{1}{2} \ln \left(\frac{p + p_z}{p - p_z} \right) = -\ln \left(\tan \frac{\theta}{2} \right).$$

The pseudorapidity distribution $dN/d\eta$ is also approximately invariant when $p \gg m$ and $\theta \gg 1/\gamma$. The advantage of the pseudorapidity to the rapidity is that it can be measured even the mass of the particle is unknown.

In the CDF, transverse energy E_T is frequently used since it is also invariant under z-boost. E_T is defined as,

$$E_T \equiv E \sin\theta$$

where E is the energy cluster observed in the calorimeter and the θ is a polar angle of a vector to the center of the energy cluster from an actual interaction point.

2.2 Tracking detectors

Tracking is important for identification of charged leptons. Since both electrons and photons leave similar signals in the calorimeter, the existence of particle track which matches to the energy cluster is an important evidence for the electron signal.

Tracking information also gives a momentum of a charged particle under the magnetic field. The CDF has a superconducting solenoidal magnet which produces 1.4 T magnetic field in the central rapidity region. This strong magnetic field enables the central tracking chamber to provide a precise momentum determination for charged particles.

Another important information provided by the tracking is an decay point of the long lived particle produced by the $p\bar{p}$ collision. This information plays a crucial role to identify those long-lived particles such as b-hadrons, which is a subject of the analysis in the thesis.

The CDF has four separate tracking detectors within the magnetic field as shown in Fig. 2.1. The outline of each detector is briefly described in the following sections.

Silicon Vertex detector: SVX

The SVX [17, 18] is a r-ϕ tracking device placed very close to the beam pipe. The main purpose of the SVX is to measure trajectories of charged particle precisely enough to distinguish b hadron decays using their relatively long decay length ($c\tau \sim 430\mu m$).

The SVX is divided into two modules at the $z = 0$ and each of half are called 'barrel'. An SVX barrel is shown in Fig. 2.3. Each barrel consists of four concentric layers of silicon micro strip sensors. The inner and outer layers of the SVX are at radii of 2.86 cm and 7.87 cm, respectively. Total length of the SVX along z axis is 51 cm (25.5cm for a barrel) and this

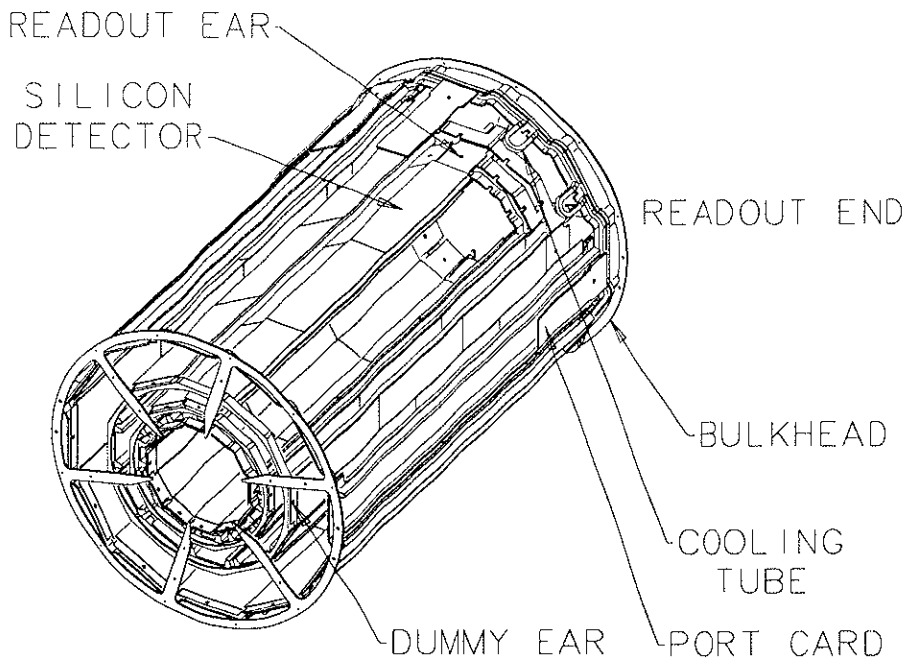

Figure 2.3: An isometric view of the SVX detector. $r = 7.9\ cm$, $l = \pm 25.5\ cm$.

length covers about 60% of $p\bar{p}$ interactions observed at the CDF.

Each of silicon sensors in a barrel have $60\mu m$ strips ($55\mu m$ for the fourth layer) along z axis on the one side. Signals from those strips are read out though 200 nm layer of S_iO_2 to prevent saturation of the input amplifier from leakage currents in the detector. The individual hit resolution is obtained by fitting the charge distribution of neighboring strips, and the resolution is about $10\mu m$.

In the thesis, SVX plays a key role to extract b-quark events from inclusive electron sample. The SVX provides a precise measurement of the impact parameter which reflects the lifetime of the parent particle.

Vertex Time Projection Chambers: VTX

The VTX consists of 28 time projection chambers which are mounted end-to-end along the z-axis. Each of the chambers have a central high voltage grid in r-ϕ plane that make the chamber to have two drift region with 4 cm

long. Drift electrons move along z-axis toward multiple sense wires arranged in r-ϕ plane, concentric to the beam axis. Those wires provide r-z view of the track by measuring the arrival times of drift electrons using Time-to-Digital Converter (TDC). The r-ϕ tracking is also provided by cathode pads behind those wires.

The VTX has a very wide acceptance in polar angles ($3.6°<\theta<176.4°$) and this enables us to determine z positions where hard $p\bar{p}$ collisions occurred. Knowledge of the location of the event vertex gives the first order correction in the calculation of physics quantities such as the transverse energy and also gives separation of multiple events in a single bunch crossing.

Central Tracking Chamber: CTC

The Central Tracking Chamber (CTC) [19] is a 1.3 m radius 3.2 m long cylindrical drift chamber which gives precise momentum measurements ($\delta p_T/p_T \sim 0.002 p_T$) in the angular region, $40°<\theta<140°$ ($-1<\eta<1$).

The CTC has 84 layers of sense wires, which are basically strung along z-axis. Those layers are grouped into 9 *super-layers*. A superlayer consists of a single layer of drift cells (*super-cells*) that surround the z-axis. Each super-cell has multiple wires to form the electric field inside. The CTC has two kinds of superlayers which alternatively surround the z-axis as shown in Fig. 2.4. The first ones which start from the innermost layer are called *axial superlayers* and whose wires are strung exactly along z-axis. The axial superlayers provide r-ϕ view of the track. The CTC has 5 such axial superlayers. The rest superlayers (4 layers) are called *stereo superlayers* and whose wires are strung with an angle of $\pm 3°$ relative to z-axis. The combined analysis of the information from the stereo superlayers and the axial superlayers provide r-z view of the track.

In each superlayer, super-cells are not arranged in parallel to the radial

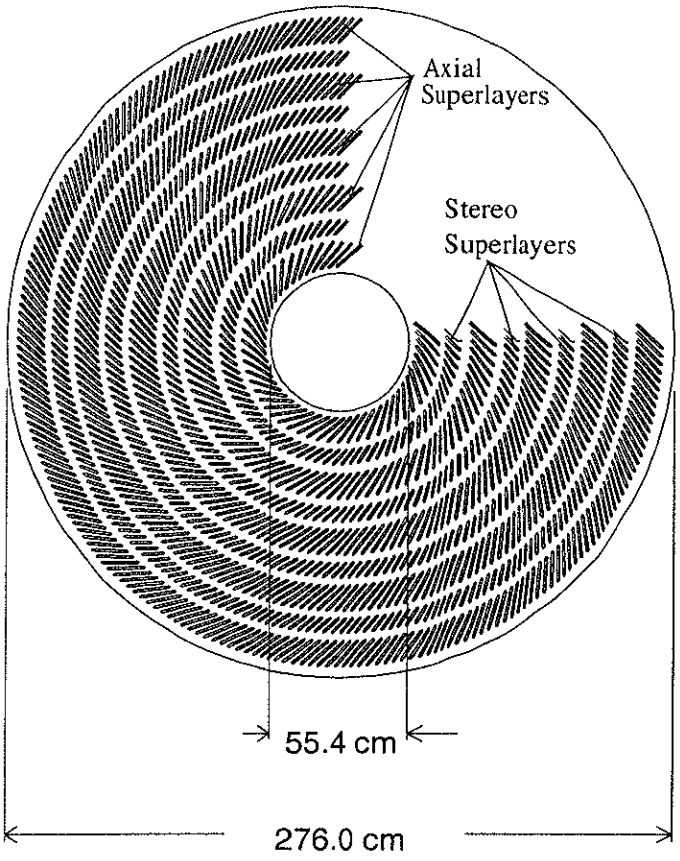

Figure 2.4: The CTC end-plate showing the wire slots.

Number of layers	84
Number of superlayers	9
Stereo angle	0° +3° 0° −3° 0° +3° 0° −3° 0°
Number of cells/layer	30 42 48 60 72 84 96 108 120
Number of sense wires/layer	12 6 12 6 12 6 12 6 12
Sense wire spacing	10 mm in plane of wires
Tilt angle(center of plane)	45°

Table 2.1: Mechanical parameters of the CTC

direction. They are tilted 45° respect to the radial direction so that the drift trajectories of electrons are approximately azimuthal under the crossed magnetic and electric field. Without this tilt angle, dead space would emerge at the ends of the cells because of a large Lorentz angle. The tilt angle of the cells has an extra advantages of resolving tracks. Since the cells do not have a mirror symmetry respect to the radial plane, the track coming from the center of the CTC can be uniquely resolved.

The CTC wire gives an extra information for the particle identification aside from the track information. The pulse height of the wire signal reflects a magnitude of the energy deposition in the drift chamber. Since the energy deposition is a function of a velocity rather than the momentum, it is possible to extract the mass of the particle by combining the observed momentum and energy deposition. In the thesis, energy deposition (=charge deposition) in the CTC is represented by Q_{CTC} and used to help separating an electron in the analysis.

2.3 Calorimeters

The main purpose of the calorimeter is to measure the magnitude and the direction of all energy flow [1] from an interaction point. One of the advantage of the calorimeter is its ability to identify the particular type of particles, i.e.

[1]Except for neutrinos and muons since they deposit no or very small part of their energy in a dense material. The muon is detected with a muon chamber.

electrons and photons, using their characteristic signature of electromagnetic cascade in a dense material. An electromagnetic cascade is caused by a chain reaction of an electron-positron pair creation by a photon which is created by a bremsstrahlung of electrons(positrons). The calorimeter to measure the energy of the electromagnetic shower is called the electromagnetic (EM) calorimeter.

The energy of the hadron can also be measured using a shower in a dense material but a strong interaction take a important part of the developing process in this case. The shower development by a strong interaction is much slower than electromagnetic shower as a function of material depth. For this reason, the calorimeters to measure hadronic energies need to have a larger depth than the EM calorimeter and it is located behind the EM calorimeters.

The CDF calorimeters use projective tower geometry, which points back to the nominal interaction point. Those towers cover the pseudo-rapidity range from -4.2 to 4.2, and cover full range in the azimuthal angle as shown in Fig. 2.5.

We use the central electromagnetic calorimeter (CEM) to tag the electron from b-hadron decay, and the forward calorimeter (FCAL) to detect the rapidity gap signature of pomeron exchange events.

Central Electromagnetic Calorimeter: CEM

The central electromagnetic calorimeter (CEM) [20] and the central electromagnetic shower max counter (CES) are the important tools to identify the electron production in the central rapidity region. They also provide the 'central electron' trigger.

The CEM covers the pseudorapidity range from -1.1 to 1.1 and has the full coverage in ϕ using 478 projective towers. The size of a tower is $0.1(\eta) \times$

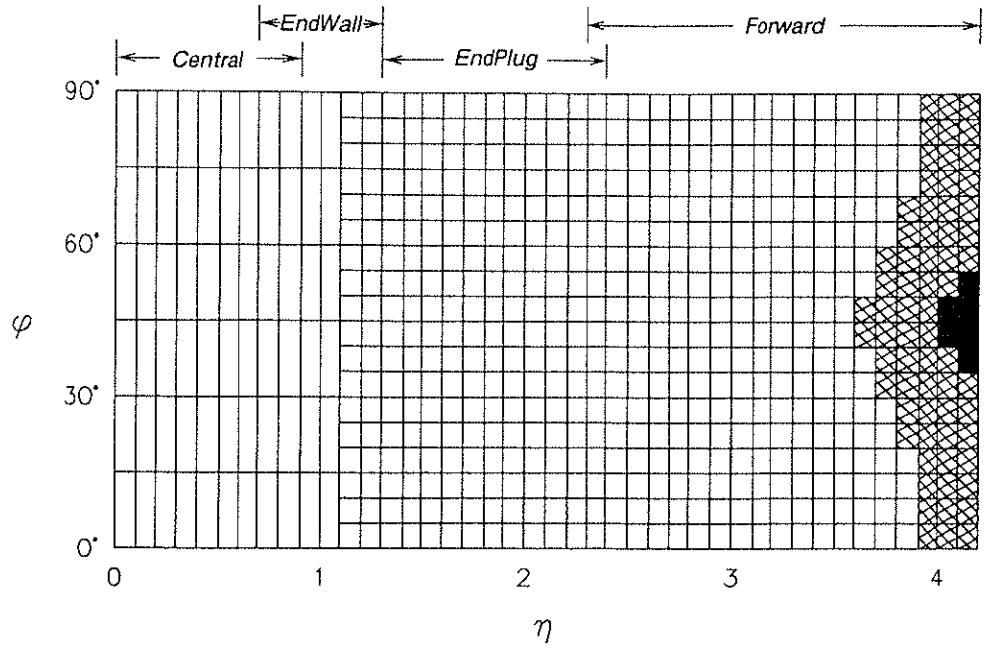

Figure 2.5: The CDF calorimeter segments shown in $\eta - \phi$ plane. Hatched area shows partial depth coverage only due to cut for low beta quadrupoles. Black area shows no coverage.

$15°(\phi)$ $(24.1cm \times 46.2cm)$ and this size is large enough to cover a typical electromagnetic shower development of a few cm in lateral size. The depth of a tower is 18 radiation length (0.6 absorption length). The CEM uses lead sheets interspersed with scintillator as the active detector medium. The scintillation light from the scintillators in a tower is collected and piped into the photomultiplier (PMT) through the wavelength-shifter. The CEM have an electron energy resolution of σ/E=13.5%/$\sqrt{E_T}$ $\oplus$2% (the symbol $\oplus$ signifies that the constant term is added in quadrature in the resolution and E_T is in GeV).

The CES is embedded at the depth of 5.9 radiation length in the CEM measured from the solenoidal coil. The longitudinal shower development becomes maximum at this depth in average. The CES is a proportional gas chamber to measure the position and the lateral shape of the electromagnetic shower at the maximum development. The CES is made up with strips

	CES chamber		CPR chamber
	Wires (r-ϕ view)	Strips (z view)	Wires (r-ϕ view)
Number of channels	32	69[a],59[b]	16
Spacing (cm)	1.45	1.67[a],2.07[b]	2.2
Spatial resolution (cm)	0.2	0.2	-
Saturation energy (GeV)	150	150	>150
Chamber length in z (cm)	234		103
Chamber width in ϕ (°)	14.0		12.1

[a]For CES segment between 6 cm $< z <$115 cm.
[b]For CES segment between 115 cm $< z <$240 cm.

Table 2.2: Description of the shower max detector (CES) and preshower detector (CPR).

perpendicular to the beam axis and wires along the beam axis. It measures the shower position in twodimensions with the resolution of 2 mm(r-ϕ:wire)$\times$ 2 mm(z:strip).

Central and Endwall Hadron Calorimeters: CHA,WHA

The central hadronic calorimeter (CHA) [21] lays after CEM, covering $|\eta|$ up to 0.9. It is mounted around the solenoid consisting of steel plates and acrylic scintillator. Because the CHA is placed in outer radius, it covers the pseudorapidity range $|\ \eta\ | < 0.9$, with the end-wall hadron calorimeter (WHA) extending this coverage out to $|\ \eta\ | < 1.3$. The CHA consists of 32 layers of 1 cm thick scintillator interleaved with layers of 2.5 cm thick steel. The WHA is made up of 15 layers of 5 cm thick steel followed by 1 cm thick scintillator. It presents 4.5 absorption lengths of material and has an energy resolution of $75\%/\sqrt{E} \oplus 3\%$.

Forward Electromagnetic Calorimeter: FEM

The forward electromagnetic calorimeter (FEM) [22] is placed at $\sim$ 6m away from the nominal interaction point in the z-direction to provide the informa-

tion of electromagnetic energy flow in the small angle region near the beam line. Two FEM are placed in the forward and the backward of the CDF. The FEM covers the pseudorapidity range from 2.3 to 4.2 ($11^\circ > \theta, \pi - \theta > 2^\circ$) and has the full coverage in azimuthal angle.

The FEM is a sandwich calorimeter of 30 lead ($96\%P_b$,$6\%S_b$) sheets and 30 proportional gas chambers. The depth of the detector is 25.5 X_0. The FEM is physically divided into quadrants at the x-z and y-z plane. The cathode pads of the chamber layers are ganged in the longitudinal direction in order to form the projective tower geometry of the unit of $0.1(\eta) \times 5^\circ(\phi)$. The tower has two depth segmentations both of which are 15 layers thick. The anode wires of chamber do not form a tower as pads, but they are ganged in each layer to form the sectors. The quadrant has 5 sectors per layers, and those sectors are read out independently for each layer.

The anode information of individual layers is not used for energy measurement itself, but used to reject the hit of slow neutron which mimic the unexpectedly high energy signal in a tower [23]. The slow neutron can kick out a slow proton in a detector, and the ionization energy loss of a slow proton is extremely larger than the one for the relativistic proton. Since a slow proton cannot go through the lead radiator layer, the high dE/dx signal is observed only in a single anode layer.

Forward Hadron Calorimeter: FHA

The forward hadron calorimeter (FHA) [24] measures the hadronic energy flow in the small angle region. It is placed behind the FEM and those two calorimeters provide a comprehensive energy measurements for this rapidity region, $2.2 < |\eta| < 4.2$. The structure of the FHA is similar to the FEM. It is a sandwich calorimeter of 27 steel plates and 27 ionization chambers. The FHA is also divided into quadrants, and the cathode pads in the chamber form

the projective tower geometry with the unit of $0.1(\Delta\eta)\times5°(\Delta\phi)$. The anode wires in each chamber layer form six sectors. The signal from those wires can be used to independently monitor the performance of the calorimeter and to provide information on the longitudinal development of showers in the detector.

In the analysis of the thesis, FEM and FHA are used to tag the rapidity gap signal in this forward rapidity region.

2.4 Central Preshower chamber: CPR

The central preshower chamber (CPR) is a multi-wire proportional chamber placed between the the CEM and the solenoid magnet coil. It samples the electromagnetic showers that started in the solenoid magnet material ($1.075X_0$). It has 2.22 cm cells segmented in r-ϕ and are positioned at a radius of 168 cm from the beam line. It consists of four chamber divisions spanning ±1.1 units of pseudo rapidity η.

In the electron identification, the CPR provides the useful information to separate the real electrons from the hadrons which mimic the electron signal in the CEM. An electron tends to start making a shower in the solenoid and thus leave a large pulse in the CPR, while a hadron tends to leave only a minimum-ionizing pulse.

2.5 Beam-Beam Counter: BBC

The beam-beam counter (BBC) consist of a set of scintillator hodoscopes mounted around the beam pipe at ~6 m from the nominal interaction point. The east and west BBCs cover the pseudorapidity range $3.24< |\eta| <5.89$ ($0.317° < \theta < 4.47°$, $0.317° < \pi - \theta < 4.47°$). The east BBC covers the positive η range, and the west BBC covers the negative. The BBC is used as the primary luminosity monitor. It also provides a relatively unbiased

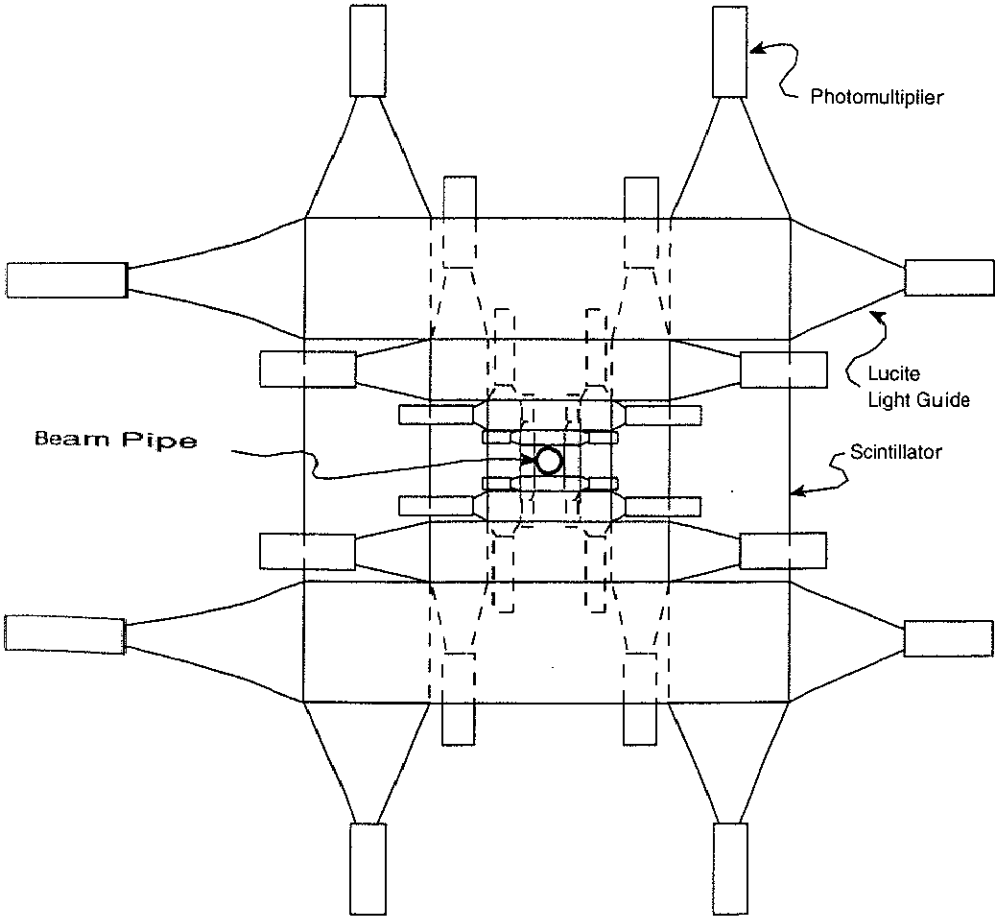

Figure 2.6: BBC counter.

"minimum-bias" trigger.

The arrangement for the BBCs is shown in Fig. 2.6. Each set of counters consists of 2 layers of scintillators; the layer closest to z=0 being mounted horizontally and the other layer being mounted vertically. Their sizes are adjusted so that they subtend roughly equal amounts of rapidity ($\Delta\eta$ ~0.67). Each scintillator is viewed by a phototube at each end.

In the thesis, the BBC is used as an important tool to tag the rapidity gap signal in addition to the forward calorimeters.

2.6 Trigger

In the CDF, the cross section for the inelastic events which at least hit the BBC in both sides is **50mb**. On the other hand, the cross section for more interesting events, for example $W \rightarrow e\nu$ is only $\mathbf{2 \times 10^{-6} mb}$. It is thus crucial for the experiment to implement the sophisticated trigger into the detector complex.

The CDF employs a three-level trigger system [25, 26]. The idea behind the multi-level trigger structure is to minimize the deadtime and to give a flexibility for the system. Several kinds of triggers are implemented in each level and the event is selected if it passes at least on of those triggers in each level. The only those relevant to the analysis are described below.

Level-1

The Level-1 decision is made within the 3.5μsec between beam crossings and it therefore incurs no deadtime. In this level, the decision is made with the simple information such as energy deposition in the calorimeter, the coincidence of east and west BBCs and the existence of the stiff track in the chamber (but no their positions). Neither no energy clustering nor no tracking is made.

The central calorimeter consists of projective towers of $0.1(\eta) \times 15°(\phi)$. In order to reduce the number of signals, the logical trigger tower of $0.2(\eta) \times 15°(\phi)$ is produced by summing the analog outputs from adjacent two towers. The electromagnetic and the hadronic towers are individually treated in the trigger. The analog signal from the trigger tower is corrected for a bias level and a gain variation, and then converted into a transverse energy by giving a $\sin\theta$ weight according to the tower position. All those correction are made in the analog stage. The trigger tower E_T is compared with certain threshold levels provided by programmable Digital-to-Analog Converter. The main Level-1 trigger which accepts the central electrons is the one using E_T threshold of 8.0 GeV for the EM energy. When a particular analog signal is over this threshold, the event is passed into the Level-2 stage.

Level-1 delivers a rate of a few kHz to the next level.

Level-2

In this stage, topological features, such as energy clusters and tracks, are reconstructed and used for the event selection. This process needs $\sim 20\mu$sec and incurs about 5$\sim$10% deadtime.

The hardware energy clustering in the calorimeter is performed using the analog signals from trigger towers. A list of the cluster properties, including position, width, and transverse energy is compiled. The hardware track reconstruction is also performed using the CTC outputs but only for r-ϕ plane [27]. Results of those reconstruction are analyzed by fast computation modules specialized to select each subjects; jets, electrons, muons and so on. The "electron" events are selected based on the cluster width, the ratio of electromagnetic to hadronic energy deposition and the presence of a high p_T track. In RUN1B, the new hardware trigger which implements the CES information was also used for electron selection [28].

Level-3

When the event passes the level-2 trigger, the entire information from the CDF detector is digitized and readout by the front end scanners. After finishing readout, the level-1 and the level-2 systems are released to evaluate the next events again. The readout data are reformed into a standard format for the offline analysis and then pushed into one of the buffers in the level-3 trigger system. The Level-3 trigger is a software trigger running on UNIX machines. The system consists of 96 buffers and 48 nodes which process the events in parallel. The electron selection in this stage is based on almost the same information as used in the offline analysis. We will describe this event selection criteria in the next chapter. The event which passes Level-3 trigger is recorded on the 8 mm tape at a rate of about 10 Hz.